

# Human Vitamin K Epoxide Reductase and Its Bacterial Homologue Have Different Membrane Topologies and Reaction Mechanisms\*<sup>♦</sup>

Received for publication, July 24, 2012, and in revised form, August 23, 2012. Published, JBC Papers in Press, August 24, 2012, DOI 10.1074/jbc.M112.402941

Jian-Ke Tie<sup>1</sup>, Da-Yun Jin, and Darrel W. Stafford

From the Department of Biology, University of North Carolina at Chapel Hill, Chapel Hill, North Carolina 27599-3280

**Background:** The membrane topology and the role of certain cysteines in human vitamin K epoxide reductase (VKOR) are disputed.

**Results:** VKOR has three transmembrane domains, and only the active site cysteines are required for function.

**Conclusion:** Despite similarities, VKOR and its bacterial homologues (VKORHs) have different topologies and reaction mechanisms.

**Significance:** The VKOR does not employ the intramolecular electron transfer pathway proposed for VKORH.

Vitamin K epoxide reductase (VKOR) is essential for the production of reduced vitamin K that is required for modification of vitamin K-dependent proteins. Three- and four-transmembrane domain (TMD) topology models have been proposed for VKOR. They are based on *in vitro* glycosylation mapping of the human enzyme and the crystal structure of a bacterial (*Synechococcus*) homologue, respectively. These two models place the functionally disputed conserved loop cysteines, Cys-43 and Cys-51, on different sides of the endoplasmic reticulum (ER) membrane. In this study, we fused green fluorescent protein to the N or C terminus of human VKOR, expressed these fusions in HEK293 cells, and examined their topologies by fluorescence protease protection assays. Our results show that the N terminus of VKOR resides in the ER lumen, whereas its C terminus is in the cytoplasm. Selective modification of cysteines by polyethylene glycol maleimide confirms the cytoplasmic location of the conserved loop cysteines. Both results support a three-TMD model of VKOR. Interestingly, human VKOR can be changed to a four-TMD molecule by mutating the charged residues flanking the first TMD. Cell-based activity assays show that this four-TMD molecule is fully active. Furthermore, the conserved loop cysteines, which are essential for intramolecular electron transfer in the bacterial VKOR homologue, are not required for human VKOR whether they are located in the cytoplasm (three-TMD molecule) or the ER lumen (four-TMD molecule). Our results confirm that human VKOR is a three-TMD protein. Moreover, the conserved loop cysteines apparently play different roles in human VKOR and in its bacterial homologues.

Vitamin K epoxide reductase (VKOR)<sup>2</sup> is a 163-amino acid polytopic membrane protein of the endoplasmic reticulum

(ER) (1, 2). It is responsible for the conversion of vitamin K 2,3-epoxide (KO) into vitamin K and is highly sensitive to inhibition by coumarin drugs, such as warfarin, the most commonly prescribed oral anticoagulant (3). Warfarin inhibition of VKOR reduces the availability of vitamin K hydroquinone (KH<sub>2</sub>), which is a cofactor for  $\gamma$ -glutamyl carboxylase.  $\gamma$ -Glutamyl carboxylase catalyzes the functionally critical post-translational modification of a family of vitamin K-dependent proteins involved in blood coagulation, bone homeostasis, signal transduction, and cell proliferation (4, 5). Deficiency of KH<sub>2</sub> causes partial carboxylation or noncarboxylation of vitamin K-dependent proteins resulting in defects primarily of blood coagulation (4, 6, 7). Concomitant with carboxylation, KH<sub>2</sub> is oxidized to KO, which must be converted back to KH<sub>2</sub> by VKOR and an as yet unidentified vitamin K reductase for the carboxylation reaction to continue.

Based on a chemical model study, a reaction mechanism for converting KO to vitamin K by VKOR was proposed by Silverman (8). A quantum chemical study of the reaction mechanism of KO reduction by VKOR supports and extends the Silverman mechanism (9). This study predicts that once a key disulfide bond of VKOR is broken, the reaction is energetically favorable. Experimental data supporting the proposed chemical model comes from a study of VKOR activity with a variety of thiol compounds (10). It has been proposed that the thioredoxin (Trx) family proteins serve as the physiological reductant for VKOR (11–14); however, this hypothesis has been questioned (15). Currently, the physiological reductant of VKOR remains unknown.

With the identification of the gene encoding human VKOR (1, 2), it became possible to study its structure-function relationship at the molecular level. Site-directed mutagenesis studies confirmed that two conserved cysteines, Cys-132 and Cys-

\* This work was supported, in whole or in part, by National Institutes of Health Grants HL077740, HL048318, and HL06350 (to D. W. S.).

<sup>♦</sup> This article was selected as a Paper of the Week.

<sup>1</sup> To whom correspondence should be addressed. Tel.: 919-962-2267; Fax: 919-962-9266; E-mail: jktie@email.unc.edu.

<sup>2</sup> The abbreviations used are: VKOR, vitamin K epoxide reductase; VKORH, vitamin K epoxide reductase homologue; VKOR-CM, charged residue

mutated VKOR; ER, endoplasmic reticulum; KO, vitamin K 2,3-epoxide; KH<sub>2</sub>, vitamin K hydroquinone; Trx, thioredoxin; FIXgla-PC, protein C with its gla domain replaced by the gla domain of FIX; FPP, fluorescence protease protection; mPEG-MAL, methoxy-polyethylene glycol maleimide; TMD, transmembrane domain; CYB5, cytochrome b<sub>5</sub>; ASGPR, asialoglycoprotein receptor; *Syn*-VKORH, *Synechococcus* vitamin K epoxide reductase homologue; PEG, polyethylene glycol; gla,  $\gamma$ -carboxyglutamic acid.

## Membrane Topology and Reaction Mechanism of VKOR

135, comprise the active site redox center (CXXC) in VKOR (16–18). Although the identity of the active site residues is clear, reports of the function of the other pair of conserved cysteines, Cys-43 and Cys-51 (the loop cysteines), do not allow a consistent interpretation for their role. Results with Trx/Trx reductase suggest that a redox protein transfers electrons to the loop cysteines, which in turn reduces the membrane-embedded active site Cys-132–Cys-135 disulfide bond to activate VKOR (19). However, a VKOR mutant with both loop cysteines changed to alanine has wild-type enzyme activity with dithiothreitol (DTT) as reductant, suggesting that the loop cysteines are not essential for VKOR activity (16, 18). We extended this observation to an *in vivo* activity assay system where VKOR uses the endogenous reductant in the native milieu rather than DTT (20). Our *in vivo* results support the conclusion that the loop cysteines are not required for VKOR activity.

To better understand the structure-function relationships of VKOR, we have determined the membrane topology of human VKOR by *in vitro* translation/co-translocation (21). Our results suggest that VKOR is a three-transmembrane domain (TMD) protein with its N terminus located in the ER lumen and C terminus in the cytoplasm (Fig. 1A). In this model, the active site cysteines (Cys-132 and Cys-135) are located at the N terminus of the third TMD facing the ER lumen. However, this topology places the conserved loop cysteines Cys-43 and Cys-51 in the cytoplasm, on the opposite side of the ER membrane from the active site cysteines. Our three-TMD model is consistent with the other results suggesting that the loop cysteines are not directly involved in VKOR activity (16, 18, 20).

VKOR appears to be a member of a large family of homologues (VKORHs) widely distributed among vertebrates, invertebrates, plants, bacteria, and archaea (22). In bacteria, VKORHs are present in strains lacking the cytoplasmic membrane protein DsbB that is important for protein oxidative folding in the periplasm (23). The functional similarity between bacterial VKORHs and DsbB is shown by the observation that bacterial VKORHs can complement DsbB to restore DsbA-dependent disulfide bond formation of secreted proteins in *Escherichia coli* (23–25). Moreover, the crystal structure of a bacterial VKORH from *Synechococcus* reveals a four-TMD structure of the VKOR domain that is similar to DsbB (26). Based on this structure, a four-TMD topology model for human VKOR has been proposed (Fig. 1B). In addition, an intramolecular electron transfer pathway between the two pairs of conserved cysteines, similar to that of DsbB, has been proposed for the bacterial VKORHs as well as for mammalian VKOR (26, 27). These results raise the question as to whether the bacterial enzymes and the mammalian ones have the same membrane topology and whether they employ different mechanisms to regenerate the active site cysteines.

To further clarify the membrane topology and the reaction mechanism of human VKOR, we employed independent biochemical techniques, fluorescence protease protection (FPP) assay (28), and selective modification of the VKOR endogenous cysteines by polyethylene glycol maleimide (PEG-MAL) (29) to probe the membrane topology of the intact VKOR molecule in mammalian cells. We used our recently established cell-based activity assay to examine the role of the conserved loop cysteines in VKOR.

Our results support the three-TMD model of human VKOR and suggest that intramolecular electron transfer between the loop cysteines and the active site cysteines of VKOR is not necessary for its function.

## EXPERIMENTAL PROCEDURES

**Materials**—Vitamin K<sub>1</sub>, warfarin, digitonin, and trypsin (bovine pancreas) were obtained from Sigma. Methoxy-polyethylene glycol maleimide, molecular weight 5000 (mPEG-MAL-5000), was purchased from Nektar (Huntsville, AL) and Laysan Bio. Inc. (Arab, AL). Luciferase substrate coelenterazine was from NanoLight Technology (Pinetop, AZ). Complete protease inhibitor mixture tablets and 2,2'-azino-bis(3-ethylbenzothiazoline-6-sulfonic acid) solution for ELISA were purchased from Roche Applied Science. Immobilon-P PVDF membrane was from Millipore Corp. (Bedford, MA). ECL Western blotting detection reagents were from GE Healthcare. Mammalian expression vector pIRESpuro3, Xfect transfection reagent, and green fluorescence protein (GFP) containing vector pEGFP-N1 were from Clontech. Cytochrome *b*<sub>5</sub> cDNA was from Open Biosystems (Huntsville, AL). The gene encoding asialoglycoprotein receptor (ASGPR) subunit H1 was kindly provided by Dr. Martin Spiess (University of Basel, Switzerland) (30). Restriction enzymes and peptide:N-glycosidase F were from New England Biolabs (Ipswich, MA). QuikChange site-directed mutagenesis kit was from Stratagene (La Jolla, CA). HEK293 cell line was from the ATCC (Manassas, VA). Mammalian expression vector pBudCE4.1, all cell culture media, and oligonucleotide primers were from Invitrogen. Mouse anti-carboxylated FIX gla domain monoclonal antibody was a gift from GlaxoSmithKline (Philadelphia) and Green Mountain Antibodies (Burlington, VT) (31, 32). Horseradish peroxidase-conjugated affinity-purified sheep anti-human protein C IgG was from Affinity Biologicals, Inc. (Ancaster, Ontario, Canada). Anti-HPC4 monoclonal antibody was from Dr. Charles T. Esmon (Oklahoma Medical Research Foundation, Oklahoma City, OK). Lab-Tek II chambered cover glasses (4-well) were from Nalge Nunc International (Rochester, NY). The 96-well enzyme immunoassay/radioimmunoassay high binding flat bottom plates were purchased from Corning Inc. (Corning, NY).

**DNA Manipulations and Plasmid Constructions**—Mammalian expression vector pIRESpuro3 was used as the basic cloning and expression vector. For the FPP assay, GFP was fused to the N or C terminus of the target protein with a 30-amino acid flexible linker (GGSGG)<sub>6</sub> between the two entities as described previously (33). The linker was generated by the annealing of four oligonucleotides with a BamHI and a BglII site flanking the 5' and the 3' end, respectively. The annealed fragment was cloned into the BamHI site of the pIRESpuro3 vector. The BglII site at the 3' end of the linker introduces an arginine residue that is susceptible to trypsin cleavage in the FPP assay. For the N-terminal GFP fusion, the gene encoding GFP was amplified by PCR using a 5' primer containing the Kozak sequence flanked by an EcoRI site and a 3' primer flanked by a BamHI site without the stop codon. The PCR product was cloned into the pIRESpuro3 vector with the (GGSGG)<sub>6</sub> linker by EcoRI/BamHI to yield pIRESpuro3-GFP-N. The gene encoding the target pro-

tein was amplified by PCR using primers flanked with an NotI site at both ends and subcloned into pIRESpuro3-GFP-N at its NotI site. For the C-terminal GFP fusion, the gene encoding GFP was amplified by PCR using primers flanked with NotI sites at both ends. The PCR product was cloned into the NotI site of the pIRESpuro3 vector with the (GGSGG)<sub>6</sub> linker to yield pIRESpuro3-GFP-C. The gene encoding the target protein was amplified by PCR using a 5' primer flanked with an EcoRI site with the Kozak sequence and a 3' primer flanked with a BamHI site (BglIII for VKOR) without the stop codon. The PCR product was subcloned into pIRESpuro3-GFP-C by EcoRI/BamHI.

For the FPP control assays, we used the single-TMD protein ASGPR and the tail-anchored protein CYB5 as model proteins. Both proteins are type II integral membrane proteins with the N terminus located in the cytoplasm and C terminus in the ER lumen. We replaced the cytoplasmic N-terminal heme-binding domain (residues 1–90) of CYB5 (34) and the luminal C-terminal carbohydrate recognition domain of ASGPR (residues 147–290) (35), respectively, with GFP (Fig. 2B).

Site-directed mutagenesis was performed by a QuikChange kit to create cysteine mutations or change the charged residues in VKOR according to the manufacturer's instructions (Stratagene). For Western blot detection, an HPC4 tag (EDQVD-PRLIDGK) was introduced at the C terminus of the VKOR with its ER retention sequence (KAKRH). As an internal control for our cell-based VKOR activity assay, *Metridia* luciferase cDNA was cloned into one of the multicloning sites of the dual mammalian expression vector pBudCE4.1 to yield pBudCE4.1-Met.Luc. All the VKOR constructs were subcloned into a different multicloning site of pBudCE4.1-Met.Luc. All the VKOR constructs for the *in vivo* cell-based activity assay have a warfarin-resistant mutation of Y139F. The nucleotide sequences of all the constructs were verified by sequencing at Eton Bioscience Inc. (Research Triangle Park, NC).

**FPP Assay**—FPP assay was performed as described previously (28) with minor modifications. HEK293 cells were subcultured into chambered cover glass with complete growth medium to yield ~80% confluency at the time for the FPP assay. Cells were transiently transfected with pIRESpuro3 plasmid DNA containing the GFP-tagged target protein using transfection reagent Xfect according to the manufacturer's protocol. Forty eight hours post-transfection, cells were washed three times for 1 min each with KHM buffer (110 mM potassium acetate, 2 mM MgCl<sub>2</sub>, and 20 mM HEPES, pH 7.2) at room temperature. After washing, 200  $\mu$ l of KHM buffer was added to each chamber before placing the chambered cover glass on the microscope stage. Confocal microscopy was performed on a Zeiss LSM710 confocal laser scanning microscope (Carl Zeiss Microimaging, Thornwood, NY). Images were collected using a 40 $\times$ /1.2NA C-Apochromat objective lens. Visualization of the GFP was achieved by use of a 488 nm argon laser line for excitation, and the detector was set to collect emission at 493–530 nm. We collected a time series of images of the chosen cell using ZEN software. Successive images were collected at an interval of 30 s. After the fourth image was taken, 200  $\mu$ l of KHM buffer containing 0.2 mM digitonin was added to the chamber (final concentration is 0.1 mM) to selectively permeabilize the plasma membrane. Two minutes after the addition of digitonin (*i.e.*

after the 8th image was taken), 400  $\mu$ l of KHM buffer containing 2  $\mu$ M trypsin was gradually added to the chamber to elicit protease digestion of GFP in the cytoplasm. The essential factor that affects the FPP assay is the concentration of digitonin. To determine the effective digitonin concentration for permeabilizing the plasma membrane, increasing concentrations of digitonin in KHM buffer were added to HEK293 cells transiently expressing GFP. The lowest digitonin concentration (0.1 mM) resulting in the disappearance of the GFP signal within 60 s was chosen (28). To compare changes in fluorescence intensity post-treatment, instrument software was used to define and mark areas of interest within cells. Mean pixel intensity within the area of interest was used as a marker for comparison.

**Selective Modification of the Endogenous VKOR Cysteines by mPEG-MAL**—Selective modification of the cysteines of VKOR by mPEG-MAL was performed as described previously (29) with additional modifications. VKOR or VKOR C43A/C51A mutant with a C-terminal HPC4 tag was transiently expressed in HEK293 cells in a 6-well plate. Forty eight hours post-transfection, cells were washed twice *in situ* with PBS, pH 6.8, and detached by pipetting. Cells were harvested by centrifugation, and cell pellets were resuspended in PBS. Samples were aliquoted into three tubes; one was a control with no detergent, and the other two were incubated with 0.1 mM digitonin or 1% Triton X-100 in the presence of a protease inhibitor mixture on ice for 10 min. The digitonin concentration used for selectively permeabilizing the plasma membrane was as described above with the GFP test in the FPP assay. Freshly prepared mPEG-MAL-5000 solution was added to each sample to a final concentration of 20 mM and incubated on ice for 30 min. The reaction was stopped by adding DTT to a final concentration of 50 mM, followed by SDS loading buffer for SDS-PAGE and Western blot detection.

**Cell-based VKOR Activity Assay**—The *in vivo* activity assay for VKOR and its variants used in this study was performed according to our recently established cell-based assay (36) with minor modifications. It is based on the ability of VKOR or its homologue to convert KO to vitamin K in mammalian cells to support the carboxylation of a reporter protein. The reporter chimera protein FIXgla-PC, which has the gla domain of factor IX replacing the gla domain of protein C, was stably expressed in HEK293 cells (FIXgla-PC/HEK293). Plasmid DNA of pBudCE4.1-Met.Luc containing the cDNA of wild-type or mutant VKOR was transiently expressed in FIXgla-PC/HEK293 cells in a 24-well plate using Xfect transfection reagent according to the manufacturer's instructions (Clontech). Five hours post-transfection, the transfection medium was replaced by a complete cell culture medium containing 5  $\mu$ M KO with 4  $\mu$ M warfarin. The cell culture medium was collected after a 48-h incubation and directly used for ELISA to determine the level of carboxylated reporter protein (FIXgla-PC) and for the luciferase activity assay to normalize for the transfection efficiency (20). Because endogenous VKOR in HEK293 cells can efficiently carboxylate the reporter protein (250–300 ng/ml carboxylated FIXgla-PC in the cell culture medium), 4  $\mu$ M warfarin was used in all assays to inhibit the endogenous VKOR activity. Warfarin reduced carboxylation of reporter protein to extremely low background levels (5–10 ng/ml carboxylated

## Membrane Topology and Reaction Mechanism of VKOR

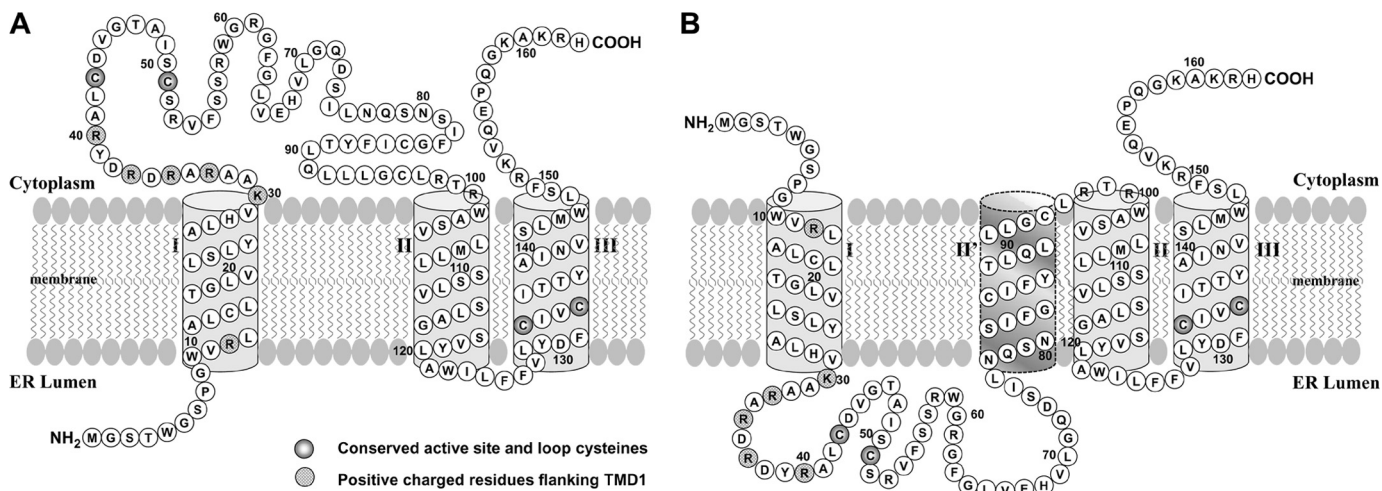


**FIGURE 1. Proposed membrane topology models of human VKOR.** *A*, three-TMD topology model of human VKOR based on *in vitro* translation/co-translocation (21). The N terminus of VKOR is located in ER lumen and the C terminus in the cytoplasm. Conserved active site and loop cysteines are indicated by gradient filling of the circle, and they are located on the opposite side of ER membrane. The positively charged residues flanking TMD1 are shaded in gray. *B*, proposed four-TMD topology model of human VKOR based on the crystal structure of a bacterial VKOR homologue (26). In this model, both the N and C termini are located in the cytoplasm. Conserved active site cysteines and the loop cysteines are located in the same side of the ER membrane.

FIXgla-PC). For this reason, all the VKOR molecules used in the cell-based activity assay have the Y139F warfarin-resistant mutation. Therefore, wild-type VKOR activity in this study refers to the activity of VKOR-Y139F warfarin-resistant mutant.

## RESULTS

**Localization of the N and C Termini of Human VKOR in HEK293 Cells by FPP Assay**—The two proposed membrane topology models for human VKOR agree with each other in terms of the location of the C terminus but are in conflict as to the location of the N terminus and the conserved loop cysteines (Cys-43 and Cys-51) (Fig. 1). To clarify this disagreement, we fused GFP to either the N or C terminus of VKOR and then used the FPP cell assays to probe the location of the two termini in intact VKOR molecules in mammalian HEK293 by confocal microscopy. These chimeric proteins were transiently expressed in HEK293 cells, and the plasma membranes were selectively disrupted by digitonin followed by the addition of trypsin. Results show that when GFP is fused to the N terminus of VKOR (GFP-VKOR), it is protected from trypsin digestion (Fig. 2A). However, the C-terminal GFP fusion of VKOR (VKOR-GFP) is susceptible to protease digestion in digitonin-permeabilized cells. This result suggests that the N terminus of VKOR is located in the ER lumen, and the C terminus is located in the cytoplasm. Control experiments were performed by fusing GFP to either the cytoplasmic or luminal terminus of the single TMD model proteins ASGPR and CYB5 (Fig. 2, B and C). These results agree with our previous *in vitro* results that suggest that VKOR is a three-TMD protein (21).

To examine the enzymatic activity of the GFP tagged VKOR molecules, we used our recently established cell-based activity assay (36). Fig. 3 shows that the fusion of GFP, which is approximately twice the size of VKOR, to VKOR decreased its activity to about 50% compared with the wild-type enzyme. This result demonstrates that the GFP-tagged VKOR used in the FPP assay for the membrane topology study has passed ER quality control and is enzymatically active.

**Selective Modification of the Endogenous Cysteine Residues in VKOR by mPEG-MAL**—Another difference between the three- and four-TMD models for VKOR is the location of the cysteine residues in terms of the ER membrane (Fig. 1). In the three-TMD model, the conserved loop cysteines Cys-43 and Cys-51 along with Cys-85 and Cys-96 are located in the cytoplasm. In contrast, none of the cysteine residues are located in the cytoplasm in the four-TMD model. To clarify these two topology models, we used a membrane-impermeable sulfhydryl modification reagent mPEG-MAL-5000 to selectively modify the cysteines of VKOR in HEK293 cells. Modification of each cysteine by mPEG-MAL-5000 is expected to increase the apparent molecular mass of VKOR by  $\geq 10$  kDa (29), which can be easily separated by SDS-PAGE and visualized by Western blot analysis. In this experiment, we transiently expressed HPC4-tagged VKOR in HEK293 cells. The cells were again treated with digitonin which preferentially permeabilizes the cell membrane over the ER membrane. Thus, the modification reagent should react only with the cysteine residues exposed to the cytoplasm. If VKOR is a four-TMD protein, none of the seven endogenous cysteines should be available to react with mPEG-MAL because they would be found within the protected ER membrane or lumen.

Fig. 4A shows that when cells expressing wild-type VKOR are selectively permeabilized by digitonin and modified by mPEG-MAL-5000, two PEG-labeled protein bands with a higher molecular weight are observed (Fig. 4A, lane 2). This result suggests that at least two cysteine residues of VKOR are located in the cytoplasm. When both the plasma and ER membranes are disrupted with Triton X-100, at least five PEG-modified protein bands are observed, and most of the VKOR molecules have two or three mPEG-MAL modifications (Fig. 4A, lane 3). Because the PEG molecule is large, when two cysteines are close to each other (for example cysteine 132 and 135), they may not be modified efficiently. In addition, when more cysteines are modified, it may decrease the transfer efficiency of the modified protein from the gel to the membrane. Our result suggests that

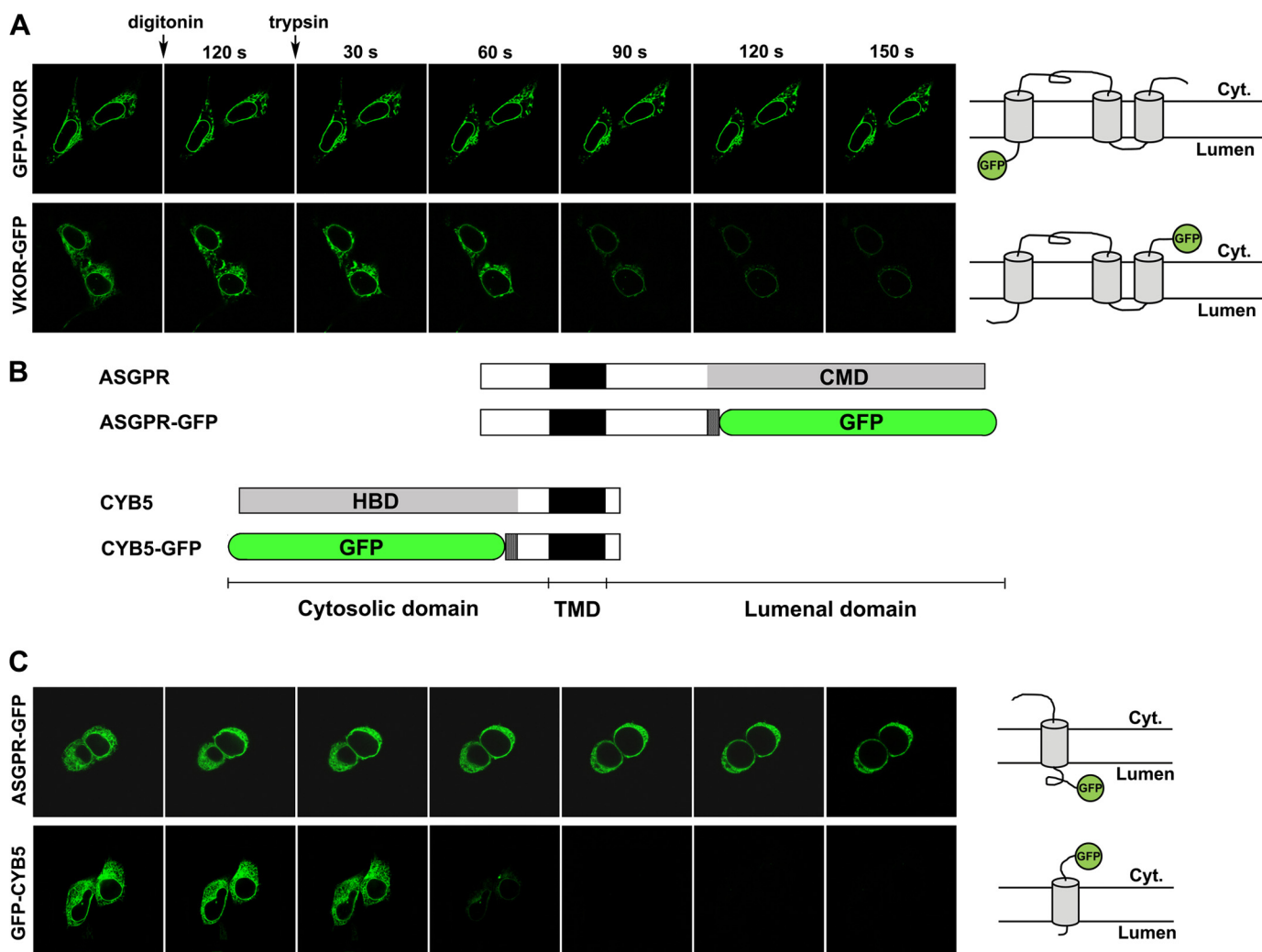


**FIGURE 2. Localization of the N and C termini of VKOR in HEK293 cells by fluorescence protease protection assay.** *A*, FPP assay of GFP fusions of human VKOR. GFP-tagged VKOR fusions were transiently expressed in HEK293 cells. Forty eight hours post-transfection, cells were selectively permeabilized with 0.1 mM digitonin. Then trypsin was added, and images were collected at the indicated time intervals. *B*, schematic representation of the single TMD model proteins (ASGPR and CYB5) and their GFP fusions. The *solid bars* indicate the TMD; the *gray bars* indicate the luminal carbohydrate recognition domain (CMD) of ASGPR or the cytoplasmic heme-binding domain (HBD) of CYB5. *Dark gray bars* indicate the (GGSGG)<sub>6</sub> linker between GFP and the model proteins. *C*, FPP assay of GFP fusion of the model proteins as described above.

at least five of the seven cysteines in VKOR can be modified simultaneously by mPEG-MAL when the plasma and ER membrane were permeabilized. These results agree with the above FFP assay and again are consistent with VKOR being a three-TMD protein.

In the three-TMD model, of the four cysteines located in the cytoplasm, Cys-43 and Cys-51 are located in a hydrophilic region, and Cys-85 and Cys-96 reside in a hydrophobic region of VKOR (Fig. 4*B*). Therefore, we suspected that the two cysteines modified under ER intact conditions (Fig. 4*A*, *lane 2*) are the cytoplasmic hydrophilic region loop cysteines Cys-43 and Cys-51. To test this hypothesis, we mutated both cysteines to alanine and repeated the mPEG-MAL modification. When Cys-43 and Cys-51 were mutated, under ER intact conditions, the two PEG protein adducts were significantly reduced in the mutant enzyme as compared with the wild-type enzyme (Fig. 4*A*, *lane 5*). In addition, the 4- and 5-fold PEG-modified forms also dramatically decreased when the cells were treated with Triton X-100 (Fig. 4*A*, *lane 6*). We demonstrated previously

that the VKOR mutant C43A/C51A has almost wild-type enzyme activity, indicating it folds correctly and functions normally (16, 20). Together our results suggest that the conserved loop cysteines Cys-43 and Cys-51 are located in the cytoplasm and again support the three-TMD model of VKOR.

*VKOR Topology Can Be Changed by Mutating the Charged Residues Flanking TMD1*—Our results thus far suggest that, consistent with our previous conclusion, VKOR is a three-TMD protein. The orientation of the first TMD in the three-TMD model agrees with the “positive inside rule” (37). A number of positively charged residues are found after the TMD1 that are located on the cytoplasmic side of the ER membrane (inside). To test the contribution of the charged residues flanking TMD1 to VKOR topology, we removed four positively charged residues at the C terminus of TMD1 by making the following mutations: K30L, R33G, R35G, and R37G. We also added three positive charged residues to the N terminus of VKOR by making the mutations of G6R, S7R, and G9R. The topology prediction program TMHMM predicts three TMDs

## Membrane Topology and Reaction Mechanism of VKOR

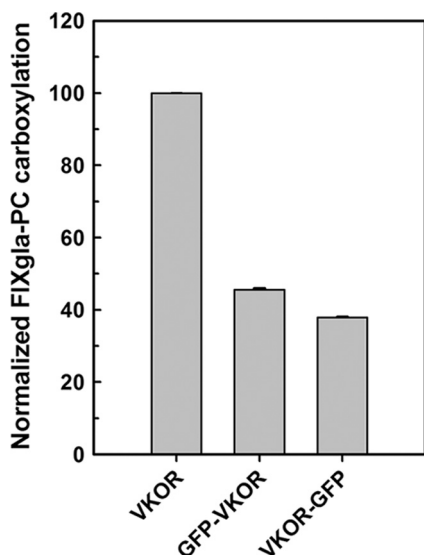


FIGURE 3. *In vivo* cell-based activity assay of human VKOR and its GFP fusions used in FPP assay. Human VKOR and its GFP fusions were transiently expressed in FIXgla-PC/HEK293 cells. Transfected cells were cultured in complete medium containing 5  $\mu\text{M}$  KO and 4  $\mu\text{M}$  warfarin for 48 h. The concentration of carboxylated FIXgla-PC in the cell culture medium was measured by ELISA and normalized by the luciferase activity as described under "Experimental Procedures." Data are presented as mean  $\pm$  S.D. ( $n = 3$ ).

for wild-type VKOR but four TMDs for the charge mutant VKOR-CM with both its N and C termini located in the cytoplasm.

To experimentally test the membrane topology of this charged residue mutant protein, we repeated the FPP assay by fusing GFP to either the N or C terminus of the VKOR-CM mutant. Our result shows that GFP fused to either the N or C terminus of VKOR-CM is now sensitive to protease digestion when the cell membrane is disrupted with digitonin (Fig. 5A). This result indicates that both ends of this mutated VKOR are located in the cytoplasm. Therefore, the membrane topology of the mutated protein has been changed to a four-TMD protein. The sequence 75–97, which we previously demonstrated could function as a stop-transfer sequence *in vitro* (21), now appears to span the membrane as a TMD. Therefore, instead of changing the topology of the whole protein, the C-terminal half of the molecule retains the orientation as in the wild-type enzyme. Compared with the C-terminal tagged GFP, there is an  $\sim 60$ -s delay in the disappearance of the fluorescence signal of the N-terminal GFP-tagged VKOR-CM. But compared with wild-type VKOR, the accessibility of the N-terminal GFP tag to protease digestion is obvious (Fig. 5B) indicating its cytoplasmic location.

To determine the enzymatic activities of the above mutant VKOR, we performed our *in vivo* cell-based activity assay. The results in Fig. 5C show that VKOR-CM mutant has an even higher activity than the wild-type enzyme. This experimentally altered four-TMD human VKOR retains almost full activity when GFP is fused to the N terminus. The C-terminal GFP fusion, however, shows significantly decreased activity. Even this VKOR mutant fusion (VKOR-CM-GFP) has almost the same activity as the wild-type nonfusion enzyme.

*Conserved Loop Cysteines Cys-43 and Cys-51 Are Not Involved in Intramolecular Electron Transfer*—The above results suggest that human VKOR normally has three TMDs. This places the conserved loop cysteines Cys-43 and Cys-51 on the opposite side of the ER membrane from the active site CXXC. Changing the charged residues flanking TMD1 reverses the orientation of TMD1 and places the loop cysteines in the ER lumen. Furthermore, the charge-mutated VKOR-CM with four TMDs appears to be more active than the wild-type enzyme. One possible reason for the higher activity of VKOR-CM could be that moving the loop cysteines to the same side (luminal) of the ER membrane as the active site CXXC favors the electron transfer pathway proposed for bacterial VKORH and human VKOR (19, 26, 27). To test this possibility, we mutated the loop cysteines (both individually and together) of the VKOR-CM mutant and tested their activity in our cell-based *in vivo* activity assay. Mutation of Cys-43 significantly decreased the VKOR activity as in the wild-type enzyme (Fig. 6). However, C51A or the double cysteine mutant (C43A/C51A) had a minor effect on VKOR activity. In addition, the activity of both the C51A and the double cysteine mutant (C43A/C51A) of the altered four-TMD form of VKOR are more active than the wild-type three-TMD enzyme. These results suggest that the increased activity in the charged residue mutant VKOR-CM is not due to the favorable location of the conserved loop cysteine for intramolecular electron transfer.

*Sequences Following the Conserved Loop Cysteine Appears Not to be Involved in the Control Mechanism for VKOR Activity*—The crystal structure of VKOR bacterial homologue revealed a 1/2-helix structure after the second conserved loop cysteine, Cys-56 (26). According to the sequence homology, these authors proposed a similar 1/2-helix (residues Ser-52 to Ser-57) in human VKOR following the second conserved loop cysteine Cys-51 that forms an amphipathic lid on the four-helix bundle. They suggested that "the 1/2-helix must move out of the way, perhaps by sliding parallel to the plane of the membrane, to allow Cys-56 in the loop to gain access to Cys-130 of the CXXC motif. In the resting state, the 1/2-helix would shield the active site, preventing it from nonselectively oxidizing proteins in the periplasm" (26). If this hypothesis holds for human VKOR, disruption of the 1/2-helix should leave the active site of VKOR open and susceptible to nonselective oxidation. In that case, VKOR (oxidized form) should be inactive. To test this hypothesis, we have mutated the conserved residue Val-54, which resides in the middle of the proposed 1/2-helix (26) to proline (Fig. 7A), a residue that should break the  $\alpha$ -helix structure. Our *in vivo* cell-based activity assay shows that this mutant protein has similar activity as wild-type VKOR (Fig. 7B). Therefore, the proposed 1/2-helix following the conserved loop cysteines of human VKOR appears not to function as a control mechanism as proposed for its bacterial homologue (26).

## DISCUSSION

VKOR is an ER membrane protein that reduces KO to vitamin K and is the target of warfarin. Although the membrane orientation of the C terminus of VKOR is not in doubt, the

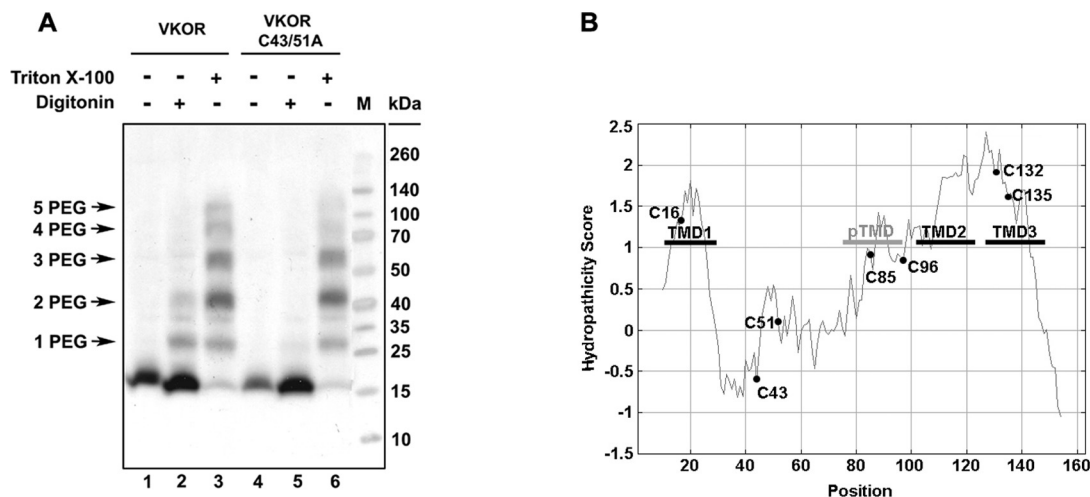


FIGURE 4. **Selective modification of the endogenous cysteine residues of human VKOR and its C43A/C51A cysteine mutant by mPEG-MAL-5000.** *A*, C-terminal HPC4-tagged VKOR or its C43A/C51A mutant was transiently expressed in HEK293 cells. Forty eight hours post-transfection, cells were harvested and permeabilized with digitonin or Triton X-100 before mPEG-MAL modification. Whole cell lysate were applied to SDS-PAGE and transferred to PVDF membrane; HPC4-tagged VKOR was analyzed by Western blot. *B*, hydropathicity profile of VKOR and the location of the endogenous cysteine residues. Transmembrane regions determined by *in vitro* translation/co-translocation were marked as TMD1 to TMD3. The putative transmembrane region was marked as pTMD in gray.

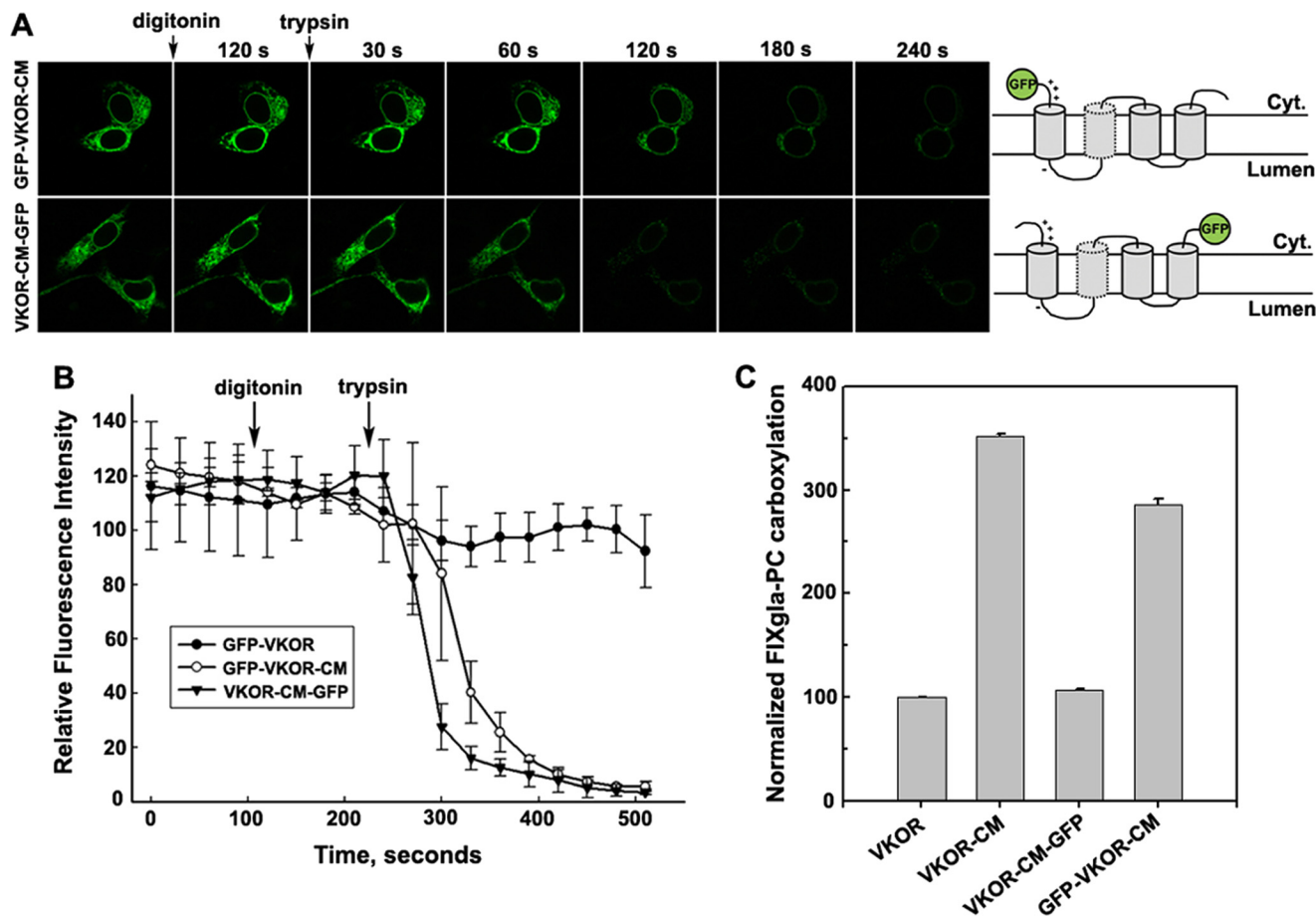


FIGURE 5. **FPP topology assay and *in vivo* cell-based activity assay of charged residue-mutated VKOR.** *A*, FPP topology assay of charged residue-mutated VKOR, VKOR-CM, as described in the legend to Fig. 2. *B*, time course of relative fluorescence intensity in FPP assay of GFP fusions of VKOR-CM compared with the N-terminal GFP fusion of wild-type VKOR. *C*, cell-based activity assay of charged residue mutated VKOR and its GFP fusions as described in the legend for Fig. 3.

number of membrane-spanning domains and the orientation of the N terminus of VKOR have been a source of contention. We presented a three-TMD model derived from *in vitro* glycosyla-

tion mapping indicating that the N terminus of VKOR is located in the ER lumen (21). However, a four-TMD model based on the crystal structure of the bacterial VKOR homo-

## Membrane Topology and Reaction Mechanism of VKOR

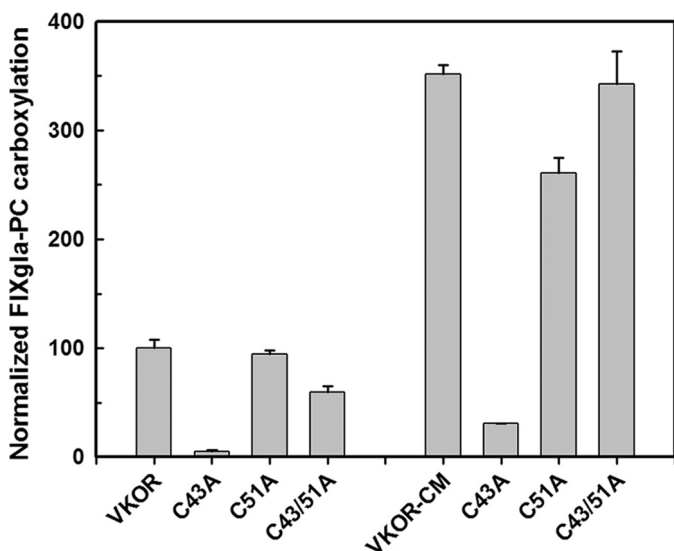


FIGURE 6. *In vivo* cell-based activity assay of the cysteine mutants of human VKOR and VKOR-CM. Cysteine mutants of VKOR or VKOR-CM were transiently expressed in FIXgla-PC/HEK293 cells, and the enzymatic activity was determined as described in the legend to Fig. 3.

logue suggests that the N terminus is located in the cytoplasm (26). These two topology models of VKOR place the conserved loop cysteines (Cys-43 and Cys-51) on different sides of the ER membrane. The location of these loop cysteines is critical for understanding the mechanism of VKOR. Our objective in this study is to address the topology and reaction mechanism discrepancy of human VKOR.

To experimentally re-examine the membrane topology of human VKOR, we used two independent biochemical approaches to probe the intact VKOR molecule in living cells. One is a recently established FPP assay that has been successfully used for determining the membrane protein topology in single cells (38). Unlike *in vitro* translation studies, where ER-derived microsomes are used as the source of cellular membranes, the FPP assay surveys proteins that are delivered by the cellular machinery to their correct destination. In addition, all the VKOR fusions used in this study for the FPP assay are active as evidenced by results from the cell-based *in vivo* activity assay. The other approach is the widely used selective modification of cysteines in the membrane protein by PEG-MAL (29). We also extended this selective modification to mammalian cells that overexpress the functional human VKOR or its cysteine mutant. Our results from both the FPP assay and selective cysteine modification support our previous conclusion that human VKOR is a three-TMD protein (Figs. 2 and 4).

It is worth noting that selective modification of cysteine residues to define the membrane topology of human VKOR has also been used in a recent study by Schulman *et al.* (27). However, these authors reported results that they interpreted as supporting the four-TMD model of VKOR. This is the only direct evidence to support the four-TMD model of human VKOR. These authors state the following: "Each cysteine modified by Mal-PEG is expected to increase the molecular weight of VKOR by ~5 kDa." While explaining their results, they state the following: "With wild-type VKOR, little modification was observed. However, extensive modification was observed when

the ER membrane was solubilized with Triton X-100, as expected from the presence of multiple endogenous cysteines located inside the ER membrane and in the ER lumen" (27). Based on the work of Lu *et al.* (29) and our results (Fig. 4), one would expect modification of multiple cysteines in a protein to result in multiple gel bands with different sizes representing different extents of cysteine modification, rather than one band with different intensities (see Fig. 1B in Ref. 27).

In addition, in that study, a cysteine residue was introduced either into the N terminus (S3C) or the C terminus (G158C) of VKOR (27). The N-terminal cysteine mutant VKOR (S3C) modification shows an increased intensity of a PEG-modified VKOR band after Triton X-100 treatment compared with digitonin treatment (Fig. 1B, compare lane 7 with lane 5 in Ref. 27). With the C-terminal cysteine mutant VKOR (G158C) modification, however, the intensity of the PEG-modified VKOR band in the sample treated with digitonin is similar to that treated with Triton X-100 (Fig. 1B, compare lane 9 with lane 11 in Ref. 27). If the two cysteines were on the same side of the membrane as in the four-TMD model, one would expect the same degree of modification for either the N- or C-terminal cysteine mutant VKOR with digitonin treatment. However, the accessibility and the relative reactivity of the two added cysteines may be different at the N or C terminus. For that reason, it appears that their results could be interpreted to support the three-TMD as well as the four-TMD topology model for VKOR.

The main difference between the two proposed topology models for VKOR is the orientation of the first TMD in the ER membrane (Fig. 1). It has been shown that the orientation of the transmembrane helix is primarily determined by the charged residues flanking the hydrophobic core, the positive inside rule that applies to both bacterial and mammalian membrane proteins (37, 39), *i.e.* positively charged residues are more abundant on the cytoplasmic side (inside) of membrane proteins as compared with the luminal/periplasmic side. Because the four-TMD topology model of human VKOR derives from the crystal structure of the VKORH of *Synechococcus* (*Syn*-VKORH), we compared the charge distribution flanking TMD1 of human VKOR and *Syn*-VKORH. The net charge difference  $\Delta(C-N)$  between the C- and N-terminal flanking regions of human TMD1 according to the rules by Hartmann *et al.* (39) is +1.5. By contrast, *Syn*-VKORH has a net charge difference of -3.5 between the C and N termini of TMD1. Thus, these two proteins have a very different distribution of charged residues flanking TMD1. According to the positive inside rule, the N terminus of VKOR should be located in the ER lumen, consistent with the three-TMD model. However, the N terminus of *Syn*-VKORH should be located in the cytoplasm, which agrees with the four-TMD topology model derived from its crystal structure. The overall charge distribution of these two proteins in their own topology model is consistent with the positive inside rule (Fig. 8A). If VKOR had four TMDs as proposed from its bacterial homologue, the charged residue distribution flanking TMD1 and the putative TMD2 would violate the positive inside rule (Fig. 8B). Therefore, deduction of the membrane topology of human VKOR from its bacterial VKORH may not be appropriate.

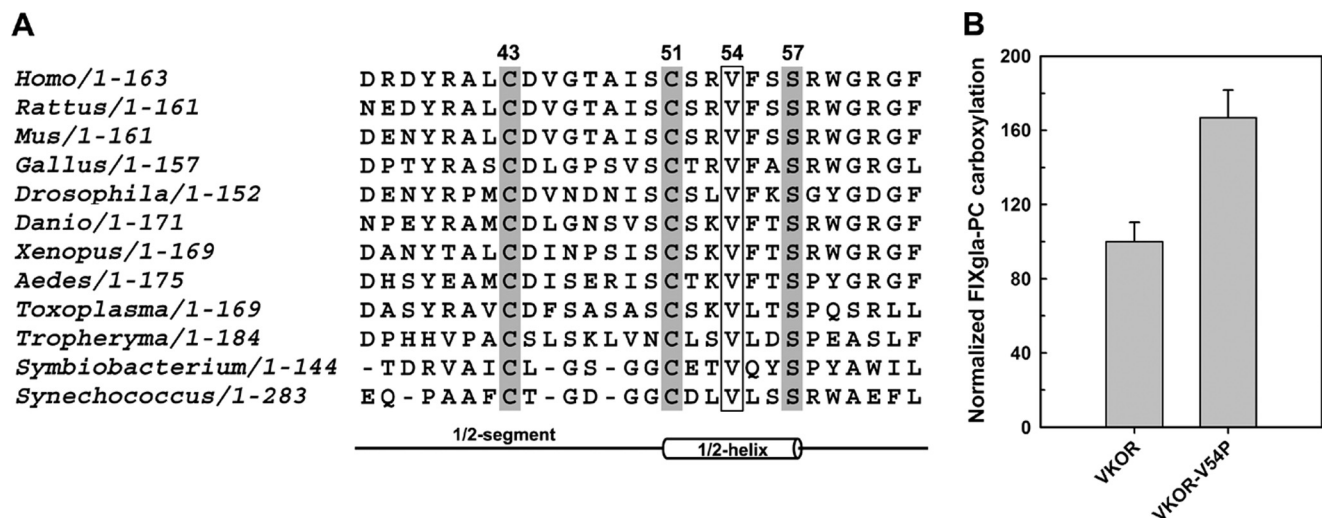


FIGURE 7. *In vivo* cell-based activity assay of human VKOR and its V54P mutant. *A*, sequence alignment of VKORs from different species per Ref. 26. Sequences were truncated between TMD1 and TMD2 as in the four-TMD topology model. Conserved loop cysteines and conserved serine are highlighted in gray. The conserved valine in the middle of the 1/2-helix is boxed. The numbers at the top refer to the position of amino acid residues in the human VKOR sequence. *B*, human VKOR and its V54P mutant were transiently expressed in FIXgla-PC/HEK293 cells, and the enzymatic activity was determined as described in the legend to Fig. 3.

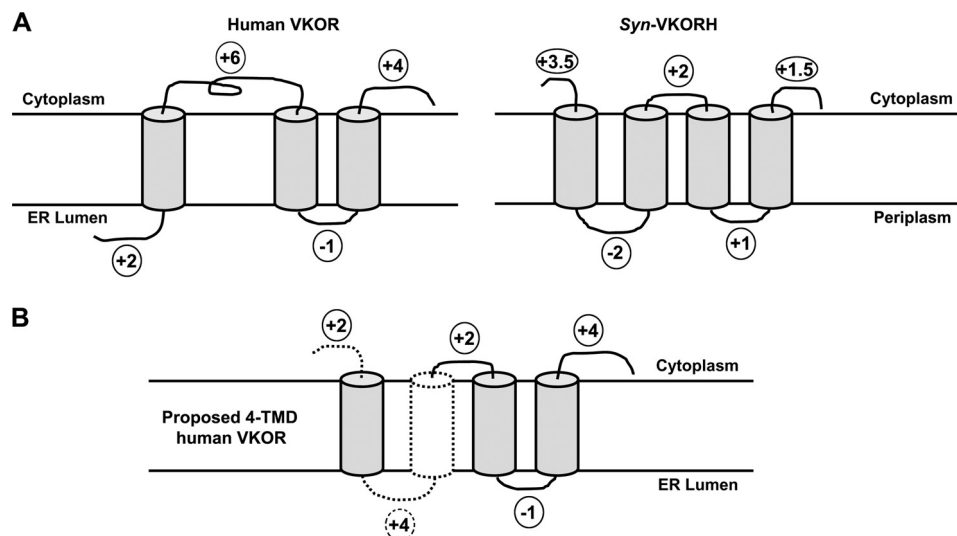


FIGURE 8. Charge distribution of human VKOR and Syn-VKORH in the proposed topology models. *A*, net charge distribution in the three-TMD model of human VKOR and the four-TMD model of the VKOR domain of Syn-VKORH. Net charges of the loops and the termini are calculated according to the rules by Hartmann *et al.* (39) and are indicated inside the circle. Arginine, lysine, and the N-terminal amino group were given a value of +1, histidine +0.5, and aspartate and glutamate -1 as described previously. *B*, net charge distribution in the proposed four-TMD model of human VKOR. The putative TMD that functions as an authentic TMD in the four-TMD variant is shown in light gray with dotted line.

It has been shown that mutating the charged residues flanking a signal sequence can invert the orientation of the peptide in the membrane (40). To further test the contribution of the positive inside rule in VKOR topology, we made charged residue mutations around the first TMD of human VKOR (VKOR-CM). The topology prediction program TMHMM predicts that the membrane orientation of TMD1 has been inverted, and this VKOR-CM mutant has been changed to a four-TMD molecule with the C-terminal half of the molecule staying the same as in the three-TMD form. FPP assays confirmed that VKOR-CM has both the N and C terminus facing to the cytoplasm. Interestingly, this molecule is even more active than the wild-type enzyme. One possible explanation for the increased activity in the four-TMD human VKOR-CM is that changing the orientation of TMD1 may change the warfarin sensitivity of VKOR.

Several residues responsible for warfarin resistance have been identified in the loop region following TMD1. These residues are located in the cytoplasm of the wild-type enzyme, but they are located in the ER lumen in the VKOR-CM mutant. This topological difference may alter warfarin sensitivity resulting in an apparent increase in VKOR activity because we include warfarin in the cell culture medium of our cell-based activity assay to inactivate the endogenous VKOR.

The other major difference in our data compared with other publications concerns the role of the loop cysteines. The loop cysteines are conserved essentially over all the known VKOR molecules. Thus, there seems little doubt that they serve an important function. It is clear that the role of the conserved loop cysteines in bacterial VKORH is to transfer electrons to the active site cysteines (24–26). Because of the homology

## Membrane Topology and Reaction Mechanism of VKOR

between human and bacterial VKORs, it was reasonable to assume that the corresponding loop cysteines, Cys-43 and Cys-51 of human VKOR, have a similar function as VKORH in bacteria.

Nevertheless, biochemical data suggest that the two conserved loop cysteines are not required for human VKOR activity (16, 18). These results agree with the three-TMD model because the loop cysteine and the active site are located at the opposite side of the ER membrane. These earlier studies were based on the *in vitro* VKOR activity assay that used DTT, which could bypass the role of the endogenous reductant. Recently, experiments using a cell-based assay, where VKOR uses its endogenous reductant, showed that the loop cysteines are not required for VKOR activity (20). Even when the loop cysteines are located on the same side of the ER membrane as the active site cysteines (Fig. 6, *VKOR-CM*), these two cysteines appear not to be involved in VKOR activity. Interestingly, the *Mycobacterium tuberculosis* VKOR homologue has four TMDs in its VKOR domain with its loop cysteines located in the periplasm. These loop cysteines are clearly required for complementation of DsbB in *E. coli* (25) but are not essential for its function in reducing vitamin K or KO in mammalian cells (20). Therefore, the conserved loop cysteines in VKOR appear not to be required for the reduction of KO in the vitamin K cycle.

Based on the crystal structure of a bacterial VKORH, it has been proposed that in human VKOR there is a "1/2-segment" in the region of the conserved loop cysteines and a "1/2-helix" immediately after this segment (Fig. 7A) (26). The 1/2-helix is proposed to serve as a control mechanism to protect the enzyme-active site. Results from this study (Fig. 7) and our previous study (16) show that deleting part of the proposed 1/2-segment or disrupting the proposed 1/2-helix has only a minor effect on VKOR activity, and this suggests that human VKOR and its bacterial homologue have different reaction mechanisms.

In conclusion, we studied the membrane topology of human VKOR by two independent approaches in mammalian cells. Our results support the three-TMD topology model of VKOR, which is consistent with the positive inside rule. We have shown that VKOR topology can be changed by changing the charged residue distribution flanking the first TMD. Cell-based *in vivo* activity assays show that the conserved loop cysteines are not essential for VKOR activity, whether they are located in the cytoplasm or the ER lumen. Together, our results indicate that human VKOR and its bacterial homologues have different membrane topologies and different mechanisms for electron transfer.

*Acknowledgments*—We thank Dr. Martin Spiess from University of Basel, Switzerland, for critical discussions and providing the cDNA of ASGPR. We thank Dr. David Straight for helping to write and organize the manuscript. We also thank Dr. Gunnar von Heijne from Stockholm University, Sweden, for useful discussions and Dr. Tony Perdue for the help on confocal fluorescence microscopy.

### REFERENCES

1. Rost, S., Fregin, A., Ivaskевичius, V., Conzelmann, E., Hörtnagel, K., Pelz, H. J., Lappegard, K., Seifried, E., Scharer, I., Tuddenham, E. G., Müller, C. R., Strom, T. M., and Oldenburg, J. (2004) Mutations in VKORC1 cause warfarin resistance and multiple coagulation factor deficiency type 2. *Nature* **427**, 537–541
2. Li, T., Chang, C. Y., Jin, D. Y., Lin, P. J., Khvorova, A., and Stafford, D. W. (2004) Identification of the gene for vitamin K epoxide reductase. *Nature* **427**, 541–544
3. Kamali, F., and Wynne, H. (2010) Pharmacogenetics of warfarin. *Annu. Rev. Med.* **61**, 63–75
4. Danziger, J. (2008) Vitamin K-dependent proteins, warfarin, and vascular calcification. *Clin. J. Am. Soc. Nephrol.* **3**, 1504–1510
5. Stafford, D. W. (2005) The vitamin K cycle. *J. Thromb. Haemost.* **3**, 1873–1878
6. Schurgers, L. J., Cranenburg, E. C., and Vermeer, C. (2008) Matrix Gla-protein. The calcification inhibitor in need of vitamin K. *Thromb. Haemost.* **100**, 593–603
7. Pauli, R. M., Lian, J. B., Mosher, D. F., and Suttie, J. W. (1987) Association of congenital deficiency of multiple vitamin K-dependent coagulation factors and the phenotype of the warfarin embryopathy. Clues to the mechanism of teratogenicity of coumarin derivatives. *Am. J. Hum. Genet.* **41**, 566–583
8. Silverman, R. B. (1981) Chemical model studies for the mechanism of vitamin K epoxide reductase. *J. Am. Chem. Soc.* **103**, 5939–5941
9. Davis, C. H., Deerfield, D., 2nd, Wymore, T., Stafford, D. W., and Pedersen, L. G. (2007) A quantum chemical study of the mechanism of action of vitamin K epoxide reductase (VKOR) II. Transition states. *J. Mol. Graph. Model.* **26**, 401–408
10. Lee, J. J., and Fasco, M. J. (1984) Metabolism of vitamin K and vitamin K 2,3-epoxide via interaction with a common disulfide. *Biochemistry* **23**, 2246–2252
11. Soute, B. A., Groenen-van Dooren, M. M., Holmgren, A., Lundström, J., and Vermeer, C. (1992) Stimulation of the dithiol-dependent reductases in the vitamin K cycle by the thioredoxin system. Strong synergistic effects with protein disulfide-isomerase. *Biochem. J.* **281**, 255–259
12. Gardill, S. L., and Suttie, J. W. (1990) Vitamin K epoxide and quinone reductase activities. Evidence for reduction by a common enzyme. *Biochem. Pharmacol.* **40**, 1055–1061
13. Silverman, R. B., and Nandi, D. L. (1988) Reduced thioredoxin. A possible physiological cofactor for vitamin K epoxide reductase. Further support for an active site disulfide. *Biochem. Biophys. Res. Commun.* **155**, 1248–1254
14. Johan, L., van Haarlem, M., Soute, B. A., and Vermeer, C. (1987) Vitamin K-dependent carboxylase. Possible role for thioredoxin in the reduction of vitamin K metabolites in liver. *FEBS Lett.* **222**, 353–357
15. Preusch, P. C. (1992) Is thioredoxin the physiological vitamin K epoxide reducing agent? *FEBS Lett.* **305**, 257–259
16. Jin, D. Y., Tie, J. K., and Stafford, D. W. (2007) The conversion of vitamin K epoxide to vitamin K quinone and vitamin K quinone to vitamin K hydroquinone uses the same active site cysteines. *Biochemistry* **46**, 7279–7283
17. Wajih, N., Sane, D. C., Hutson, S. M., and Wallin, R. (2005) Engineering of a recombinant vitamin K-dependent  $\gamma$ -carboxylation system with enhanced  $\gamma$ -carboxyglutamic acid forming capacity. Evidence for a functional CXXC redox center in the system. *J. Biol. Chem.* **280**, 10540–10547
18. Rost, S., Fregin, A., Hünerberg, M., Bevans, C. G., Müller, C. R., and Oldenburg, J. (2005) Site-directed mutagenesis of coumarin-type anticoagulant-sensitive VKORC1. Evidence that highly conserved amino acids define structural requirements for enzymatic activity and inhibition by warfarin. *Thromb. Haemost.* **94**, 780–786
19. Rishavy, M. A., Usabalieva, A., Hallgren, K. W., and Berkner, K. L. (2011) Novel insight into the mechanism of the vitamin K oxidoreductase (VKOR). Electron relay through Cys-43 and Cys-51 reduces VKOR to allow vitamin K reduction and facilitation of vitamin K-dependent protein carboxylation. *J. Biol. Chem.* **286**, 7267–7278
20. Tie, J. K., Jin, D. Y., and Stafford, D. W. (2012) *Mycobacterium tuberculosis* vitamin K epoxide reductase homologue supports vitamin K-dependent carboxylation in mammalian cells. *Antioxid. Redox. Signal.* **16**, 329–338
21. Tie, J. K., Nicchitta, C., von Heijne, G., and Stafford, D. W. (2005) Membrane topology mapping of vitamin K epoxide reductase by *in vitro* trans-

- lation/co-translocation. *J. Biol. Chem.* **280**, 16410–16416
22. Goodstadt, L., and Ponting, C. P. (2004) Vitamin K epoxide reductase. Homology, active site, and catalytic mechanism. *Trends Biochem. Sci.* **29**, 289–292
  23. Dutton, R. J., Boyd, D., Berkmen, M., and Beckwith, J. (2008) Bacterial species exhibit diversity in their mechanisms and capacity for protein disulfide bond formation. *Proc. Natl. Acad. Sci. U.S.A.* **105**, 11933–11938
  24. Singh, A. K., Bhattacharyya-Pakrasi, M., and Pakrasi, H. B. (2008) Identification of an atypical membrane protein involved in the formation of protein disulfide bonds in oxygenic photosynthetic organisms. *J. Biol. Chem.* **283**, 15762–15770
  25. Wang, X., Dutton, R. J., Beckwith, J., and Boyd, D. (2011) Membrane topology and mutational analysis of mycobacterium tuberculosis VKOR, a protein involved in disulfide bond formation and a homologue of human vitamin K epoxide reductase. *Antioxid. Redox. Signal.* **14**, 1413–1420
  26. Li, W., Schulman, S., Dutton, R. J., Boyd, D., Beckwith, J., and Rapoport, T. A. (2010) Structure of a bacterial homologue of vitamin K epoxide reductase. *Nature* **463**, 507–512
  27. Schulman, S., Wang, B., Li, W., and Rapoport, T. A. (2010) Vitamin K epoxide reductase prefers ER membrane-anchored thioredoxin-like redox partners. *Proc. Natl. Acad. Sci. U.S.A.* **107**, 15027–15032
  28. Lorenz, H., Hailey, D. W., and Lippincott-Schwartz, J. (2006) Fluorescence protease protection of GFP chimeras to reveal protein topology and subcellular localization. *Nat. Methods* **3**, 205–210
  29. Lu, J., and Deutsch, C. (2001) Pegylation. A method for assessing topological accessibilities in Kv1.3. *Biochemistry* **40**, 13288–13301
  30. Spiess, M., Schwartz, A. L., and Lodish, H. F. (1985) Sequence of human asialoglycoprotein receptor cDNA. An internal signal sequence for membrane insertion. *J. Biol. Chem.* **260**, 1979–1982
  31. Aktimur, A., Gabriel, M. A., Gailani, D., and Toomey, J. R. (2003) The factor IX  $\gamma$ -carboxyglutamic acid (Gla) domain is involved in interactions between factor IX and factor XIa. *J. Biol. Chem.* **278**, 7981–7987
  32. Feuerstein, G. Z., Patel, A., Toomey, J. R., Bugelski, P., Nichols, A. J., Church, W. R., Valocik, R., Koster, P., Baker, A., and Blackburn, M. N. (1999) Antithrombotic efficacy of a novel murine antihuman factor IX antibody in rats. *Arterioscler. Thromb. Vasc. Biol.* **19**, 2554–2562
  33. Gutscher, M., Sobotta, M. C., Wabnitz, G. H., Ballikaya, S., Meyer, A. J., Samstag, Y., and Dick, T. P. (2009) Proximity-based protein thiol oxidation by H<sub>2</sub>O<sub>2</sub>-scavenging peroxidases. *J. Biol. Chem.* **284**, 31532–31540
  34. Brambillasca, S., Yabal, M., Makarow, M., and Borgese, N. (2006) Unassisted translocation of large polypeptide domains across phospholipid bilayers. *J. Cell Biol.* **175**, 767–777
  35. Wahlberg, J. M., and Spiess, M. (1997) Multiple determinants direct the orientation of signal-anchor proteins. The topogenic role of the hydrophobic signal domain. *J. Cell Biol.* **137**, 555–562
  36. Tie, J. K., Jin, D. Y., Straight, D. L., and Stafford, D. W. (2011) Functional study of the vitamin K cycle in mammalian cells. *Blood* **117**, 2967–2974
  37. von Heijne, G. (1989) Control of topology and mode of assembly of a polytopic membrane protein by positively charged residues. *Nature* **341**, 456–458
  38. Wunder, C., Lippincott-Schwartz, J., and Lorenz, H. (2010) Determining membrane protein topologies in single cells and high throughput screening applications. *Curr. Protoc. Cell Biol.* Chapter 5, Unit 5.7
  39. Hartmann, E., Rapoport, T. A., and Lodish, H. F. (1989) Predicting the orientation of eukaryotic membrane-spanning proteins. *Proc. Natl. Acad. Sci. U.S.A.* **86**, 5786–5790
  40. Beltzer, J. P., Fiedler, K., Fuhrer, C., Geffen, I., Handschin, C., Wessels, H. P., and Spiess, M. (1991) Charged residues are major determinants of the transmembrane orientation of a signal-anchor sequence. *J. Biol. Chem.* **266**, 973–978